Plenary session

Defective endoplasmic reticulum stress response via X box-binding protein 1 is a major cause of poor liver regeneration after partial hepatectomy in mice with non-alcoholic steatohepatitis

Katsuki Miyazaki, MD [1], Yu Saito, MD, PhD, FACS [1], Mayuko Ichimura-Shimizu, PhD [2], Satoru Imura, MD, PhD, FACS [1], Tetsuya Ikemoto, MD, PhD, FACS [1], Shinichiro Yamada, MD, PhD, FACS [1], Kazunori Tokuda, MD [1], Yuji Morine, MD, PhD, FACS [1], Koichi Tsuneyama, MD, PhD [2], Mitsuo Shimada, MD, PhD, FACS [1]

1. Department of Surgery, Tokushima University, 3-18-15 Kuramoto-cho, Tokushima, 770-8503, Japan
2. Department of Pathology and Laboratory Medicine, Tokushima University, 3-18-15 Kuramoto-cho, Tokushima, 770-8503, Japan

Correspondence: Yuji Morine

Department of Surgery, Tokushima University, 3-18-15 Kuramoto-cho, Tokushima, 770-8503, Japan.

This article has been accepted for publication and undergone full peer review but has not been through the copyediting, typesetting, pagination and proofreading process which may lead to differences between this version and the Version of Record. Please cite this article as doi: 10.1002/jhbp.1142

Phone: +81-88-633-9276, Fax: +81-88-631-9698

E-mail: **ymorine@tokushima-u.ac.jp**

Manuscript type: Plenary session

Table count: 1

Figure count: 6

Keywords: Nonalcoholic steatohepatitis, hepatectomy, liver regeneration, endoplasmic reticulum stress response, lipid droplets

Abstract

Background

Non-alcoholic fatty liver disease (NAFLD) is the most common chronic liver disease. Poor regeneration after hepatectomy in NAFLD is well recognized, but the mechanism is unclear. Endoplasmic reticulum (ER) stress plays an important role in the development of NAFLD. Here, we show that an impaired ER stress response contributes to poor liver regeneration in partially hepatectomized mice.

Methods

Non-alcoholic fatty liver (NAFL) or non-alcoholic steatohepatitis (NASH) was induced in mice using our patented feed and 70% partial hepatectomy (PH) was performed. Mice were sacrificed 0, 4, 8, 24, or 48 hours, or 7 days after PH, and liver regeneration and the mRNA expression of ER stress markers were assessed.

Results

NAFLD activity score was calculated as 4–6 points for NAFL and 7 points for NASH. NASH was characterized by inflammation and high ER stress marker expression before PH. After PH, NASH mice showed poorer liver regeneration than controls. High expression of proinflammatory cytokine genes was present in NASH mice 4 hours after PH. Xbp1-s mRNA expression was high in control and NAFL mice after PH, but no

higher in NASH mice.

Conclusions

Dysfunction of the ER stress response might be a cause of poor liver regeneration in NASH.

Background

The prevalence of non-alcoholic fatty liver disease (NAFLD) is increasing worldwide and it has become one of the most common chronic liver diseases [1]. Furthermore, NAFLD is a risk factor for both primary and metastatic liver malignancy. The liver is characterized by a strong regenerative ability, and the only curative therapy for liver cancer is hepatectomy. However, NAFLD, and especially non-alcoholic steatohepatitis (NASH), is associated with a higher risk of postoperative complications after hepatectomy, such as admission to the intensive care unit, infections, and liver failure, which is associated with a high level of mortality [1-2]. Furthermore, the incidence of post-hepatectomy mortality has also been reported to be higher in patients with NASH [1,3], and mice with fatty liver show poor liver regeneration and a lower survival rate after hepatectomy [4]. This impairment in the ability of the liver to regenerate may limit the indications for hepatectomy and reduce the incidence of cure in patients with liver cancer who have NASH. Previously, excessive oxidative stress and a disorder of autophagic flux have been reported to be potential mechanisms for the impairment in liver regeneration that characterizes NASH [5,6]. However, no studies to date have been able to fully characterize the mechanisms involved. Therefore, the identification of the mechanisms of the poor liver regeneration that characterizes NASH

and the development of appropriate therapeutic strategies are major challenges in the field of hepatobiliary surgery.

The endoplasmic reticulum (ER) stress response plays an important role in the maintenance of cellular homeostasis in the face of various types of stress [7]. There are three stress sensor pathways in the ER lumen, which involve inositol-requiring enzyme-1α (IRE-1α), PKR-like endoplasmic reticulum kinase (PERK), and activating transcription factor 6 (ATF6) [7]. Chronic ER stress is known as important factor in the onset of NAFLD, the transition to non-alcoholic steatohepatitis (NASH), and hepatocarcinogenesis [8]. Essentially, activated IRE-1α spliced unspliced form of X box-binding protein 1 (XBP-1u), and the spliced form of XBP1 (XBP-1s) contribute to cell survival by inducing the expression of genes involved in ER-associated degradation and molecular chaperones [7]. Several investigators have previously reported a relationship between the ER stress response via IRE-1α -XBP-1s axis and liver regeneration after hepatectomy, especially in early phase [9-11]. Liu *et al.* demonstrated that IRE-1α promotes liver regeneration through the regulation of the signal transducer and activator of transcription 3 (STAT3) pathway [9]. Argemi *et al.* also showed that the expression of XBP-1s is induced immediately after hepatectomy, and that this regulates the unfolded protein response, acute phase response, and DNA damage repair during

liver regeneration [10]. Hamano *et al.* reported lipid overloading during liver regeneration might be caused ER stress and results in delayed liver regeneration in simple steatosis mice [11]. On the other hands, there are only a few reports which indicate the relationship between the other ER stress pathways, PREK and ATF-6, and liver regeneration [12]. And some studies also showed only IRE-1α-XBP-1s axis has relation to liver regeneration [9-10]. Thus, dysregulation of the ER stress response, especially IRE-1α-XBP-1s axis, may explain the poor liver regeneration in patients with NASH who undergo hepatectomy.

NAFLD includes very wide disease concept, from simple steatosis to NASH, and NASH related hepatocarcinogenesis. However, many of past studies focused on NAFLD have not state which stage their models are. We already established diet induced NAFL and NASH mice model [13]. And our models reflect similar pathophysiological features of human NAFL and NASH [13]. In this study, we use our the novel NAFL and NASH mice model, and identify their similarities and differences in liver regeneration after partial hepatectomy.

In the present study, we aimed to identify the mechanism of liver regeneration in a mouse model of NAFL and NASH, focusing on the ER stress response, and the IRE-1α-XBP-1s axis in particular.

Material and Methods

Ethics declarations

The present study was conducted in compliance with the requirements of the Division for Animal Research Resources, Tokushima University. The experiments and procedures were approved by the Animal Care and Use Committee of Tokushima University.

Mice

Six-week-old male C57BL/6 mice were purchased from Charles River Laboratories Japan, Inc. (Kanagawa, Japan). They were housed at room temperature and humidity under a 12-hour dark/light cycle (lights on at 08:00) and had free access to water and feed. The mice were allocated to three groups: control, non-alcoholic fatty liver (NAFL), and NASH groups, according to the feed they consumed. Before feeding each diet, all mice were consumed standard laboratory chow for 1 week. After this period, the control mice were fed a standard diet for 10 weeks, the NAFL mice were fed a high-fat diet (HFD) containing palm oil and cholesterol (Oriental Yeast Co., Ltd. Tokyo, Japan) for 10 weeks, and the NASH mice were fed the specially developed

iHFC, which contained palm oil, cholesterol, and cholic acid (Hayashi Kasei, Osaka, Japan), and reproduces the pathophysiology of NASH, for 16 weeks. [13]. Unlike conventional models of NASH, such as the methionine and choline-deficient diet model, leptin-deficient mice, or drug-induced models, iHFC induces NASH with fibrosis without the need for genetic manipulation or a deficiency of specific nutrients [13]. Moreover, the pathogenetic mechanism of the NASH induced by this diet involves obesity and insulin resistance, which closely mirrors the pathophysiological characteristics of human NASH [13]. Therefore, we consider that this model of NASH is more suitable for the study of NASH than the more conventional models.

Surgical procedures

All the surgical procedures were performed under anesthesia that was induced and maintained using 2.0% isoflurane. Seventy-percent partial hepatectomy (PH) was performed as previously reported [14]. Briefly, a midline incision of ~2 cm was made, the falciform ligament and membranes around the left lateral lobe of the liver were dissected, and then the median and left lateral lobes were mobilized. The base of the left lateral lobe was ligated first, followed by the base of the median lobe, using 4-0 silk. The lobes were then removed, and finally the peritoneum and skin were closed using 4-

0 sutures. Subsequently, the mice were sacrificed 0, 4, 8, 24, or 48 h, or 7 days following hepatectomy (10 mice for each group for survival rate analysis, and 6 mice for each time point and each group for the other analysis). Immediately before euthanasia, cardiac blood samples were collected for biochemical analysis. The remnant liver was harvested and weighed, then one portion of the caudate lobe was placed in RNAlater (Thermo Fisher Scientific, Inc., Waltham, MA, USA) for RT-PCR and the other portion was fixed in 10% formaldehyde for histological assessment.

Liver regeneration rate

Liver regeneration was assessed using the ratio of the mass of the remnant liver (right and caudate lobes) to body mass. There are differences in both body and liver mass before hepatectomy among three groups due to the differences of their food. Thus, liver regeneration rate (LRR) was adjusted for preoperative remnant liver (right and caudate lobes) to body mass ratio of each group. LLR was calculated as LLR = (remnant liver mass after hepatectomy/body mass before hepatectomy)/(mean remnant liver-to-body mass ratio before hepatectomy).

NAFLD activity score

NAFLD activity score was assessed using Kleiner's method and hematoxylin and eosin (H&E)-stained liver sections [15], and fibrosis was scored using azan-stained samples.

Immunohistochemistry

Immunohistochemistry was performed as previously reported [16]. Anti-caspase-3 antibody (dilution 1:200, #9661; Cell Signaling Technology, Inc., Danvers, MA, USA) and anti-proliferating cell nuclear antigen (PCNA; dilution 1:3,000, #10205-2-AP; PeproTech, Inc., Rocky Hill, NJ, USA) antibody were used as the primary antibodies.

We manually counted the caspase-3-positive hepatocytes in three high-power fields (400× magnification) per mouse and calculated the mean number of caspase-3-positive hepatocytes. We also counted the number of PCNA-positive nuclei and the total number of nuclei in the hepatocytes in 3 high-power fields (200× magnification) and calculated the proportion of PCNA-positive cells.

Histological assessments were performed by two expert pathologists.

Lipid droplet count

The number of lipid droplets (LDs) was counted using the image analysis software ImageJ (National Institute of Health, Bethesda, MD, USA) [17]. High-magnification H&E-stained images were opened in Image J, and at this magnification, 5.88 pixels were equivalent to 1 μm. After excluding blood vessels, images were converted to grayscale (8 bit; green), then the areas of the LDs were calculated using minimum and maximum thresholds of 220 and 255, respectively. In the present study, we focused on large LDs, which were defined as being larger than the nuclei of the hepatocytes (~10 μm), and counted LDs with diameters ≥10 μm using the particle function. Counts were recorded as the mean values for three microscopic fields per mouse.

Real-time PCR analysis

RNA was extracted from liver tissue using RNeasy Mini Kits (Qiagen, Hilden, Germany), in accordance with the manufacturer's instructions. cDNA was synthesized using a reverse transcription kit (Applied Biosystems, Foster City, CA, USA). The following primers were used for TaqMan gene expression assays (Thermo Fisher Scientific, Inc., Waltham, MA, USA): interleukin-6 (IL-6; Mm00446190_m1), tumor necrosis factor-α (TNF-α; Mm00443528_m1), IRE-1α (Mm00470233_m1), XBP-1s

(Mm03464496_m1), unspliced XBP-1 (XBP-1u; Mm03464497_s1), hepatocyte growth factor (HGF; Mm01135184_m1), transforming growth factor-β (TGF-β; Mm01178820_m1), STAT-3 (Mm01219775_m1), fat-specific protein-27 (FSP-27; Mm01219775_m1), and glyceraldehyde 3-phosphate dehydrogenase (GAPDH; 4352339E). RT-PCR was performed using an Applied Biosystems 7500 real-time PCR system and the expression of the target genes was normalized to that of the reference gene GAPDH.

Biochemical analysis

The serum levels of alanine aminotransferase (ALT) before hepatectomy were measured by Shikoku Chuken, Inc. Kagawa, Japan.

Statistical analysis

Data are presented as the mean ± standard deviation (SD). Comparisons among the three groups were made using the Mann-Whitney U-test or ANOVA test**.** $P < 0.05$ was considered to represent statistical significance. We used JMP 8.0.1 (SAS Institute Inc., Cary, NC, USA) to perform all the statistical analyses.

Results

Evaluation of the NASH model

Reflecting the steatosis present, livers from NAFL and NASH mice were paler than those from controls (Figure. 1a). Table 1 shows the NAFLD activity scores for each group. Although steatosis and ballooning were present in liver sections from both NAFL and NASH mice, there was more severe inflammation in the NASH mice (Figure 1b). Moreover, liver fibrosis was only observed in the livers of NASH mice (Figure 1c). The NAFL and NASH mice were significantly heavier than the controls (Figure 1d), and the liver-to-body mass ratio of the NASH mice was significantly higher than those of the control and NAFL mice (Figure 1e). These findings are consistent with the pathophysiology of NAFL and NASH.

Expression of markers of inflammation and ER stress before PH

No significant differences were observed in IL-6 mRNA expression among the three groups, but the expression of TNF- α mRNA expression was high in NASH mice prior to hepatectomy (Figure 2a, b). The expression of IRE-1α and XBP-1s mRNA was lower in both the NAFL and NASH mice than in controls (Figure 2c, d), but the XBP-1s/XBP-1u mRNA expression ratio and serum ALT level were higher in the NASH mice

(Figure 2e, f). Therefore, NASH appears to be characterized by chronic ER stress.

Liver regeneration and survival rate after PH

The liver regeneration of the NASH mice was significantly poorer than that of the control mice from 24 hours after PH (Figure 3a). In contrast, the NAFL mice showed comparable liver regeneration to control mice until 48 hours after PH. However, liver regeneration was significantly worse in both the NAFL and NASH mice than in controls 1 week after PH (Figure 3a). Nevertheless, the NAFL mice had a superior LRR to the NASH mice. Reflecting their poor liver regeneration, the 1-week survival rates were only 40% for the NASH mice and 60% for the NAFL mice (Figure 3b).

Expression of growth factor genes after PH

HGF is an accelerator of liver regeneration. No significant differences were found in HGF mRNA expression among the three groups, either before or after PH (Figure 3c). In contrast, TGF-β—a negative regulator of liver regeneration—was expressed at a significantly higher level in NASH mice than in controls soon after PH (Figure 3d). This suggests that liver regeneration was inhibited in NASH mice from soon after PH.

Expression of ER stress and proinflammatory cytokine genes after PH

The proinflammatory cytokines IL-6 and TNF-α are important for the initiation of liver regeneration. The mRNA expression of both IL-6 and TNF- α was high in NASH mice 4 hours following PH (Figure 4a, b). However, no significant differences were observed in the expression of IRE-1α mRNA among the three groups after PH (Figure 4c, f). As previously reported [10], XBP-1s mRNA expression was swiftly induced by PH in control and NAFL mice (Figure 4d), but the increase in XBP-1s mRNA expression did not occur in the NASH mice (Figure 4d). Moreover, XBP-1s/XBP-u, predictor of the degree of ER stress and following UPR, increased in control and NAFL after hepatectomy (Figure 4e). However, in NASH, although XBP-1s/XBP-u was significantly higher before hepatectomy (Figure 2e), it decreased immediately after hepatectomy (Figure 4e). This result suggests that NASH may not be able to response to acute stress of hepatectomy due to chronic and uncompensated ER stress. Furthermore, STAT-3, which is downstream of XBP-1s and is involved in hepatocyte proliferation, was also expressed at a significantly lower level in the NASH mice than in controls soon after PH (Figure 4f).

Hepatocyte proliferation was assessed by immunostaining for PCNA. The

proportion of PCNA-positive hepatocytes was significantly lower in the NASH mice than in the control mice 24 and 48 hours after PH (Figure 5a). In contrast, there were more caspase-3-positive hepatocytes in the livers of the NASH mice than in those of the control or NAFL mice 24 hours after PH (Figure 5b). These results suggest that the impaired ER stress response that characterizes NASH after PH inhibits hepatocyte proliferation and induces apoptosis.

LD metabolism

In the early phase of liver regeneration following hepatectomy, LDs transiently accumulate in hepatocytes, a phenomenon that is referred to as transient regeneration-associated steatosis (TRAS) [18]. The accumulated LDs are broken down into fatty acids, which undergo β-oxidation to provide energy for liver regeneration. In the control mice, TRAS occurred from 4 hours after hepatectomy and peaked after 24 hours (Figure 6a). Microvesicular steatosis developed in the livers of control mice, but all the LDs had disappeared by 1 week following PH. In contrast, in the NASH mice, there was microvesicular steatosis before and soon after hepatectomy but, in addition, a large number of large LDs accumulated from 8 hours after PH (Figure 6a), and the size and number of these large LDs increased with time. Moreover, the large LDs remained until

the late phase of liver regeneration.

The number of large LDs of ≥10 μm was measured using Image J. Both in the NAFL and NASH mice, the numbers of large LDs increased following hepatectomy. However, the peak LD accumulation was 4 hours after hepatectomy in the NAFL mice, whereas the LD accumulation continued until 24 hours after hepatectomy in the NASH mice (Figure 6b). FSP27 is involved in the fusion and growth of LDs [19], and consistent with the LD data, its expression increased in the NASH mice (Figure 6c). These results suggest that the utilization of fatty acids as an energy source is disrupted in the NASH mice, which would imply a lack of energy supply for liver regeneration.

Discussion

In the present study, we have shown that the expression of IRE-1α and XBP-1s is downregulated in mice with NASH or NAFL, reflecting chronic ER stress, and that liver regeneration following hepatectomy in mice with NASH is impaired, perhaps because of a poor ER stress response, and specifically low XBP-1s expression. Moreover, we have also shown that there is a disorder of energy metabolism, indicated by a substantial accumulation of large LDs in the liver of mice with NASH following hepatectomy. And also, this is the first report to focused on the similarities and

differences between NAFL and NASH during liver regeneration after hepatectomy.

In NASH mice, liver regeneration rate continually decreased until 48 hours after hepatectomy. Ibis, et al. reported that liver hypertrophy depends on the extent of liver resection [20]. The death in NASH group mainly occurred within 48 hours after hepatectomy. Thus, in NASH, it seemed that liver regeneration almost did not progress and remnant liver was atrophied due to excessive liver resection and resulting severe acute liver failure.

We have also provided evidence for a role of XBP-1s and IRE-1α in liver regeneration following hepatectomy. Hamano, et al. reported mice with simple hepatic steatosis showed high expression of XBP-1s [11]. However, our NAFL and NASH model showed significantly lower expression of XBP-1s than control before hepatectomy (Figure 2d). Thus, it might be considered that the expression of XBP-1s increases in simple steatosis, and decreases with the progression to NAFL and NASH due to the uncompensated ER stress. Moreover, NASH showed significantly higher XBP-1s/XBP-1u than control and NAFL before hepatectomy (Figure 2e). Although, there are no consensus to quantify ER stress response, XBP-1s/XBP-1u has been used to predict the degree of ER stress and following UPR [21]. Thus, low expression of XBP-1s in NAFL and NASH may reflect chronic ER stress. And higher XBP-1s/XBP-

1u in NASH may represent uncompensated ER stress response. Moreover, after hepatectomy, both XBP-1s and XBP-1s/XBP-1u immediately increased in control and NAFL (Figure 4e). However, in NASH, the expression of XBP-1s did not increase, and XBP-1s/XBP-1u significantly decreased (Figure 4e). This phenomenon may reflect that NASH cloud not response to acute stress of hepatectomy, due to chronic and uncompensated ER stress.

In the present study, although hepatocyte proliferation is significantly poor in NASH, there were no significant differences in the expression of HGF among the three groups, either before or after PH (Figure 3c). In contrast, TGF-β was significantly overexpressed in NASH soon after PH (Figure 3d). HGF is known to promote liver regeneration by inducing the proliferation of hepatocytes. He *et al.* reported sustained ER stress decrease the sensitivity of hepatocytes to HGF-induced proliferation [22]. TGF- β is also known as a negative regulator of liver regeneration. Zeng *et al.* reported XBP-1s decreased TGF- β family protein secretion [23]. Taken together our results and these previous reports, chronic ER stress in NASH may contribute to poor hepatocyte proliferation by decreasing the sensitivity to HGF and increasing TGF- β expression through XBP-1s downregulation.

Although XBP-1s expression is regulated by IRE-1α during the ER stress

response, XBP-1s expression was significantly lower in the NASH mice after hepatectomy, whereas there were no significant differences in IRE-1α expression among the three groups during liver regeneration (Figure 4c, d). Argemi *et al.* reported that the expression of XBP-1s is induced immediately after hepatectomy and that IL-6 knockout mice do not show higher XBP-1s expression following hepatectomy [10]. This suggests that XBP-1s expression may be regulated not only by IRE-1α, but also by proinflammatory cytokines, such as IL-6. Moreover, Liu *et al.* reported that the induction of IkappaB kinase beta (IKKβ) expression by proinflammatory cytokines causes the phosphorylation of XBP-1s, independent of IRE-1α [24]. However, the chronic inflammation that develops alongside fatty liver leads to cytokine resistance, and therefore an inactivation of IKKβ [24]. In the present study, TNF-α expression was high in the NASH mice before hepatectomy, then that of TNF-α and IL-6 was excessively upregulated soon after hepatectomy. Thus, in NASH, a chronic ER stress response and resistance to the cytokine-induced induction of XBP-1s may develop following hepatectomy, preventing the upregulation of XBP-1s expression. STAT-3, which is downstream of XBP-1s, is involved in hepatocyte proliferation after hepatectomy [9,10] but, in the present study, the expression of STAT-3 was significantly lower in the NASH mice than in controls after hepatectomy. Furthermore, the

proportion of PCNA-positive hepatocytes was also significantly lower in the NASH mice than in controls. These findings are considered to be the result of the defective upregulation of XBP-1s in the NASH mice. In contrast, the proportion of caspase-3-positive hepatocytes was significantly higher in the NASH mice than in controls. IRE-1α has two domains: an RNase domain and a kinase domain [25]. When the Rnase domain is activated, XBP-1s is activated, which promotes cell survival [25]. In contrast, prolonged or high levels of stress activate the kinase domain, which induces apoptosis [25]. Thus, in the mice with NASH that underwent PH, the kinase domain may have been activated by a prolonged period of ER stress.

The precise energy source for liver regeneration has not been fully established. However, TRAS may be considered to be a general source of energy for liver regeneration [18]. In the normal liver, TRAS occurred after hepatectomy and all the mice accumulated LDs with microvesicular morphology in their livers. However, the accumulation of large LDs was characteristic of the NASH mice. LD catabolism in hepatocytes involves a combination of lipolysis and lipophagy. Lipolysis targets large LDs and reduces their size, and these smaller LDs are subject to lipophagy [26]. FSP-27 is important for the fusion and growth of LDs and is an inhibitor of lipolysis [27], and its expression was high at all the time points following hepatectomy in the NASH mice.

Xu et, al. reported that FSP-27 expression is upregulated by ER stress [28]. Additionally, the IRE-1α-XBP-1s axis regulates lipid metabolism [29]. IRE-1α modulates autophagy by promoting autophagosome-lysosome fusion [29], and XBP-1s binds to and activates the promoter of the peroxisome proliferator-activated receptor α (PPARα) gene, a key modulator of fatty acid oxidation [29]. Thus, the excessive accumulation of large LDs after hepatectomy in the NASH mice was likely the result of the higher expression of FSP-27 and the disruption of the ER stress response, which is thought to reflect impaired lipid utilization.

The present study had several limitations. First, we only evaluated the IRE-1α-XBP-1s axis, but ATF-6, PERK, and their downstream signals are also important for the ER stress response. They work partially cooperatively and partially independently, and their works are very complex. Although the lack of evaluation of the two pathways is a major limitation of our study, it is still worthwhile to explain the cause of liver regeneration failure in NASH via IRE-1-XBP-1 axis. Second, we did not evaluate energy metabolism in detail during liver regeneration; instead, we limited our assessment to LDs. In the future, it will be necessary to further evaluate the defect in energy production by, for example, assessing monoconidial function or morphology, fatty acid oxidation, lipophagy, and ATP turnover. Third, we focused on the early phase

of liver regeneration and demonstrated dysregulation of the ER stress response via IRE-1α-XBP-1s axis in the NASH mice. In contrast, the NAFL mice showed comparable liver regeneration to normal mice until 48 hours after PH. However, in these mice, liver regeneration was significantly worse than in the normal mice 1 week following PH. Therefore, liver regeneration in NAFL may only be impaired in the mid-to-late phases. Further studies will be required to completely elucidate the mechanism of the poor liver regeneration in NAFL and NASH. There were no significant differences among 3 groups in XBP-1s 24 hours after hepatectomy. Thus, it may be difficult to use XBP-1s as a biomarker after hepatectomy. The ratio of XBP-1s and XBP-1u was significantly elevated in NASH than both control and NAFL before hepatectomy. So, in the context of postoperative liver failure prediction, the ratio of XBP-1s and XBP-1u might be a useful biomarker. Moreover, our findings suggest that the XBP-1s may represent a therapeutic target for impaired liver regeneration after hepatectomy in patients with NASH. Chemical chaperones, PPAR agonists, and AMP-activated protein kinase agonists have been reported to modulate ER stress [30]. Furthermore, cell therapies using mesenchymal stem cells or hepatocyte-like cells differentiated from stem cells may also represent candidate therapies [31,32].

In conclusion, an impaired ER stress response, and especially dysregulation of

XBP-1s, might underpin poor liver regeneration in NASH.

Acknowledgments

This study was supported by the Support Center for Advanced Medical Sciences, Tokushima University Graduate School of Biomedical Sciences.

We thank Mark Cleasby, PhD from Edanz (https://jp.edanz.com/ac) for editing a draft of this manuscript.

Conflict of interest

The authors declare no conflict of interest for this article.

References:

1. Reddy SK, Marsh JW, Varley PR, Mock BK, Chopra KB, Geller DA, et al. Underlying steatohepatitis, but not simple hepatic steatosis, increases morbidity after liver resection: a case-control study. *Hepatology.* 2012; 56(6): 2231-30.
2. Gomez D, Malik HZ, Bonney GK, Wong V, Toogood GJ, Lodge JPA, et al. Steatosis predicts postoperative morbidity following hepatic resection for colorectal metastasis. *Br J Surg.* 2007; 94(11): 1395-402.

3. Vatelainen R, Vliet AV, Gouma DJ, Gulik TMV. Steatosis as a risk factor in liver surgery. *Ann Surg*. 2007; 245(1): 20-30.

4. Zimmers TA, Jin X, Zhang Z, Jiang Y, Koniaris LG. Epidermal growth factor receptor restoration rescues the fatty liver regeneration in mice. *Am J Physiol Endocrinol Metab.* 2017; 313(4): 440-9.

5. Haga S, Ozawa T, Yamada Y, Morita N, Nagashima I, Inoue H, et al. p62/SQSTM1 plays a protective role in oxidative injury of steatotic liver in a mouse hepatectomy model. *Antioxid Redox Signal.* 2014; 21(18): 2515-30.

6. Matsumoto Y, Yoshizumi T, Toshima T, Takeishi K, Fukuhara T, Itoh S, et al. Ectopic localization of autophagosome in fatty liver is a key factor for liver regeneration. *Organogenesis.* 2019; 15(1): 24-34.

7. Kitakaze K, Taniuchi S, Kawano E, Hamada Y, Miyake M, Oyadomari M, et al. Cell-based HTS identifies a chemical chaperone for preventing ER protein aggregation and proteotoxicity. *Elife*. 2019; 8: e43302. doi: 10.7554/eLife.43302.

8. Lebeaupin C, Vallee D, Hazari Y, Hetz C, Chevet E, Bailly-Maitre B. Endoplasmic reticulum stress signalling and the pathogenesis of non-alcoholic fatty liver disease. *J Hepatol.* 2018; 69(4): 927-47.

9. Liu Y, Shao M, Wu Y, Yan C, Jiang S, Liu J, et al. Role for the endoplasmic reticulum stress

sensor IRE1α in liver regenerative responses. *J Hepatol.* 2015; 62(3): 590-8.

10. Argemi J, Kress TR, Chang HC, Ferrero R, Bertolo C, Moreno H, et al. X-box Binding Protein 1 Regulates Unfolded Protein, Acute-Phase, and DNA Damage Responses During Regeneration of Mouse Liver. *Gastroenterology.* 2017; 152: 1203-16.
11. Hamano M, Ezaki H, Kiso S, Fukuta K, Egawa M, Kizu T, el al. Lipid overloading during liver regeneration causes delayed hepatocyte DNA replication by increasing ER stress in mice with simple hepatic steatosis. *J Gastroenterol.* 2013; 49:305-16
12. Inaba Y, Furutani T, Kimura K, Watanabe H, Haga S, Kido Y, et al. Growth arrest and DNA damage-inducible 34 regulates liver regeneration in hepatic steatosis in mice. *Hepatology.* 2015: 61(4):1343-56.
13. Ichimura-Shimizu M, Omagari K, Yamashita M, Tsuneyama K. Development of a novel mouse model of diet-induced nonalcoholic steatohepatitis–related progressive bridging fibrosis. *Biosci Biotechnol Biochem.* 2021; 85(4): 941-7.
14. Mitchell C, Willenbring H. A reproducible and well-tolerated method for 2/3 partial hepatectomy in mice. *Nat Protoc.* 2008; 3(7): 1167-70.
15. Kleiner DE, Brunt EM, Natta MV, Behling C, Contos MJ, Cummings OW, et al. Design and validation of a histological scoring system for nonalcoholic fatty liver disease. *Hepatology.* 2005; 41(6): 1313-21.

16. Miyazaki K, Morine Y, Imura S, Ikemoto T, Saito Y, Yamada S, et al. Preoperative lymphocyte/C-reactive protein ratio and its correlation with CD8 + tumor-infiltrating lymphocytes as a predictor of prognosis after resection of intrahepatic cholangiocarcinoma. *Surg Today*. 2021; doi: 10.1007/s00595-021-02295-5. [Online ahead of print].

17. Sasaki Y, Asahiyama M, Tanaka T, Yamamoto S, Murakami K, Kamiya W, et al. Pemafibrate, a selective PPARα modulator, prevents non-alcoholic steatohepatitis development without reducing the hepatic triglyceride content. *Sci Rep.* 2020; 10(1): 7818.

18. Kachaylo E, Tschuor C, Calo N, Borgeaud N, Ungethum U Limani P, et al. PTEN Down-Regulation Promotes β-Oxidation to Fuel Hypertrophic Liver Growth After Hepatectomy in Mice. *Hepatology.* 2017; 66(3): 908-21.

19. Sans A, Bonnafous S, Rousseau D, Patouraux S, Canivet CM, Leclere PS, et al. The Differential Expression of Cide Family Members is Associated with Nafld Progression from Steatosis to Steatohepatitis. *Sci Rep.* 2019; 9(1): 7501.

20. Ibis C, Asenov Y, Akin M, Azamat IF, Sivrikoz N, Gurtekin B. Factors Affecting Liver Regeneration in Living Donors After Hepatectomy. *Med Sci Monit.* 2017; 23:5986-93.

21. Lee K, Tirasophon W, Shen X, Michalak M, Prywes R, Okada T, et al. IRE1-mediated unconventional mRNA splicing and S2P-mediated ATF6 cleavage merge to regulate XBP1 in signaling the unfolded protein response. *Gened Dev.* 2002; 16(4):452-66.

22. He Y, Long J, Zhong W, Fu Y, Li Y, Lin S. Sustained endoplasmic reticulum stress inhibits hepatocyte proliferation via downregulation of c-Met expression. *Mol Cell Biochem*. 2014; 389(1-2): 151-8.

23. Zeng L, Li Y, Yang J, Wang G, Margariti A, Xiao Q, et al. XBP 1-Deficiency Abrogates Neointimal Lesion of Injured Vessels Via Cross Talk With the PDGF Signaling. *Arterioscler Thromb Vasc Biol*. 2015; 35(10): 2134-44

24. Liu J, Ibi D, Taniguchi K, Lee J, Herrema H, Akosman B, et al. Inflammation Improves Glucose Homeostasis through IKKβ-XBP1s Interaction. *Cell*. 2016; 167(4): 1052-66.

25. Kato H, Katoh R, Kitamura M. Dual Regulation of Cadmium-Induced Apoptosis by mTORC1 through Selective Induction of IRE1 Branches in Unfolded Protein Response. *PLoS One*. 2013; 8(5): e64344.

26. Schott MB, Weller SG, Schulze RJ, Krueger EW, Drizyte-Miller K, Casey CA, et al. Lipid droplet size directs lipolysis and lipophagy catabolism in hepatocytes. *J Cell Biol*. 2019; 218(10): 3320-35.

27. Sharma R, Luong Q, Sharma VM, Harberson M, Harper B, Colborn A, et al. Growth hormone controls lipolysis by regulation of FSP27 expression. *J Endocrinol*. 2018; 239(3): 289-301.

28. Xu MJ, Cai Y, Wang H, Altamirano J, Chang B, Bertola A, et al. Fat-Specific Protein 27/CIDEC Promotes Development of Alcoholic Steatohepatitis in Mice and Humans. *Gastroenterology*.

2015; 149(4):1031-41.

29. Shao M, Shan B, Liu Y, Deng Y, Yan C, Wu Y, et al. Hepatic IRE1α regulates fasting-induced metabolic adaptive programs through the XBP1s-PPARα axis signalling. *Nat Commun.* 2014; 5: 3528.

30. Jung TW, Choi KM. Pharmacological Modulators of Endoplasmic Reticulum Stress in Metabolic Diseases. *Int J Mol Sci.* 2016; 17(2): 192.

31. Hu C, Zhao L, Wu Z, Li L. Transplantation of mesenchymal stem cells and their derivatives effectively promotes liver regeneration to attenuate acetaminophen-induced liver injury. *Stem Cell Res Ther*. 2020; 11(1):88.

32. Michalik M, Głady A, Czekaj P. Differentiation of Cells Isolated from Afterbirth Tissues into Hepatocyte-Like Cells and Their Potential Clinical Application in Liver Regeneration. *Stem Cell Rev Rep*. 2021; 17(2): 581-603.

514 **Table1: NAFLD activity score among three groups**

	Steatosis	Inflammation	Ballooning	Total	Fibrosis
Control	0	0	0	0	0
NAFL	2-3	0-1	2	4-6	0
NASH	3	2	2	7	1

515

516

517 **Figure legends**

518

519 **Figure 1. Evaluation of non-alcoholic fatty liver (NAFL) and non-alcoholic**

520 **steatohepatitis (NASH) models**

521 (a) Appearance of the liver. (b) Hematoxylin and eosin-stained liver sections (×100). (c)

522 Azan-stained liver sections (×100). (d) Body mass. (e) Liver-to-body mass ratio.

523 * $P < 0.05$, ** $P < 0.01$.

524

525 **Figure 2. Expression of markers of inflammation and endoplasmic reticulum (ER)**

526 **stress prior to hepatectomy**

527 (a) Interleukin-6 (IL-6) mRNA. (b) Tumor necrosis factor-α (TNF-α) mRNA

528 expression. (c) IRE-1α mRNA expression. (d) XBP-1s mRNA expression.

529 (e) Ratio of XBP-1s to XBP-1u mRNA expression. (f) Serum alanine transaminase

530 (ALT) level.

531 * $P < 0.05$, ** $P < 0.01$.

532

533 **Figure 3. Liver regeneration after hepatectomy.**

534 (a) Liver regeneration rate (LRR). (b) Survival rate after hepatectomy. The 1-week

survival rates were 90%, 60%, and 40% for control, NAFL, and NASH mice, respectively. (n=10 for each group) (c) Hepatocyte growth factor (HGF) mRNA. (d) Transforming growth factor beta (TGF-β) mRNA.

* $P < 0.05$, $P < 0.01$.

Figure 4. Expression of markers of inflammation and endoplasmic reticulum (ER) stress after hepatectomy.

(a) Interleukin-6 (IL-6) mRNA. (b) Tumor necrosis factor-α (TNF-α) mRNA expression. (c) IRE-1α mRNA expression. (d) XBP-1s mRNA expression. (e) mRNA expression ratio of XBP-1s to XBP-1u. (f) STAT-3 mRNA expression.

* $P < 0.05$, ** $P < 0.01$.

Figure 5. Immunohistochemistry of proliferating cell nuclear antigen (PCNA) and Caspase-3.

(a) PCNA positive hepatocyte rates at 24 and 48 hours after hepatectomy.

(b) Caspase-3 positive hepatocyte counts at 24 hours after hepatectomy.

* $P < 0.05$, ** $P < 0.01$.

Figure 6. Lipid droplets (LDs) evaluation.

553 (a) hematoxylin and eosin (H&E)-stained liver sections of control and NASH. (b) Large

554 lipid droplets (≥10 μm) count. (c) Fat specific protein 27 (FSP27) mRNA expression.

555 * $P < 0.05$, ** $P < 0.01$.

Fig.1

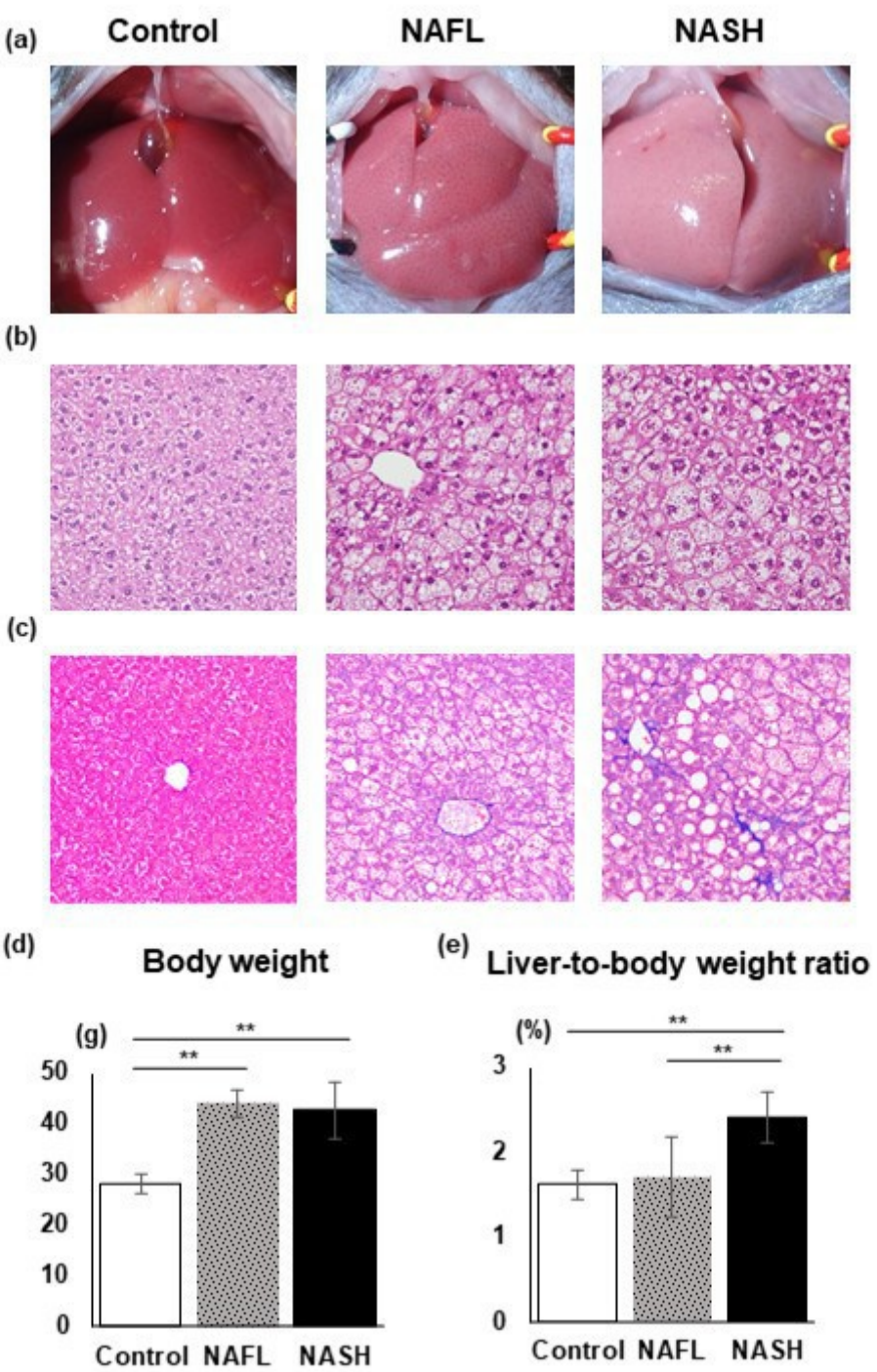

JHBP_1142_1.JPG

Fig.2

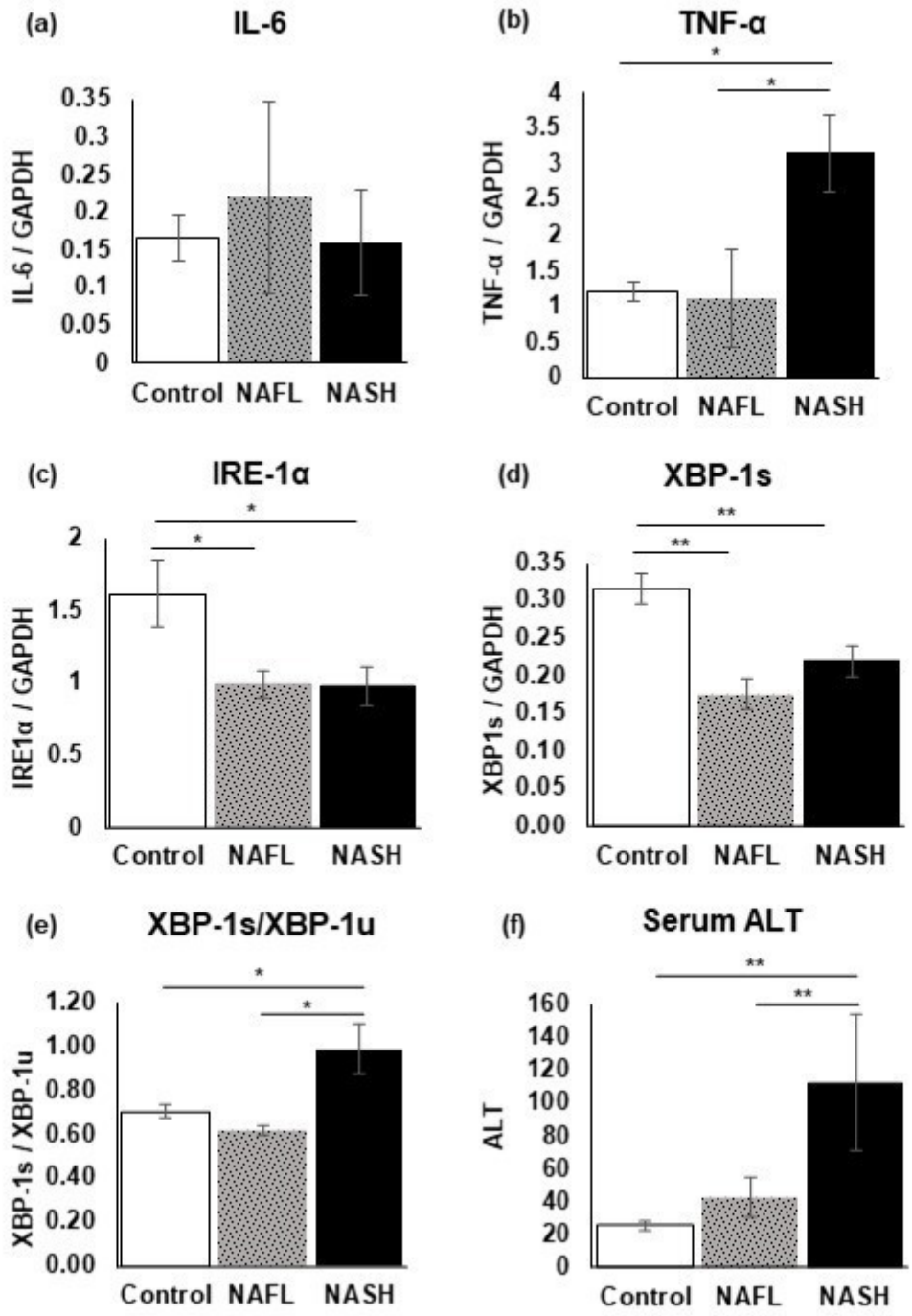

JHBP_1142_2.JPG

Fig.3

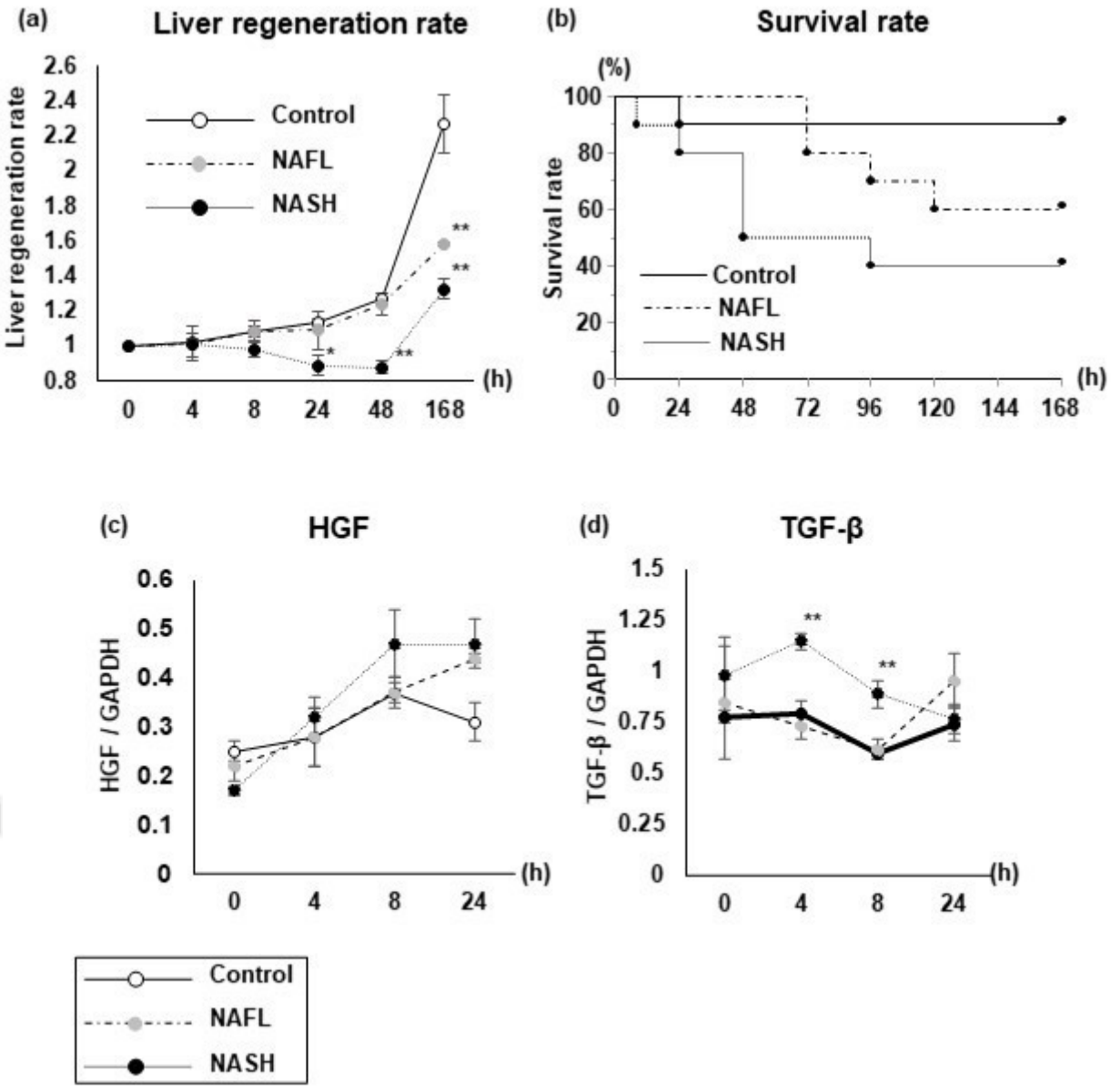

JHBP_1142_3.JPG

Fig. 4

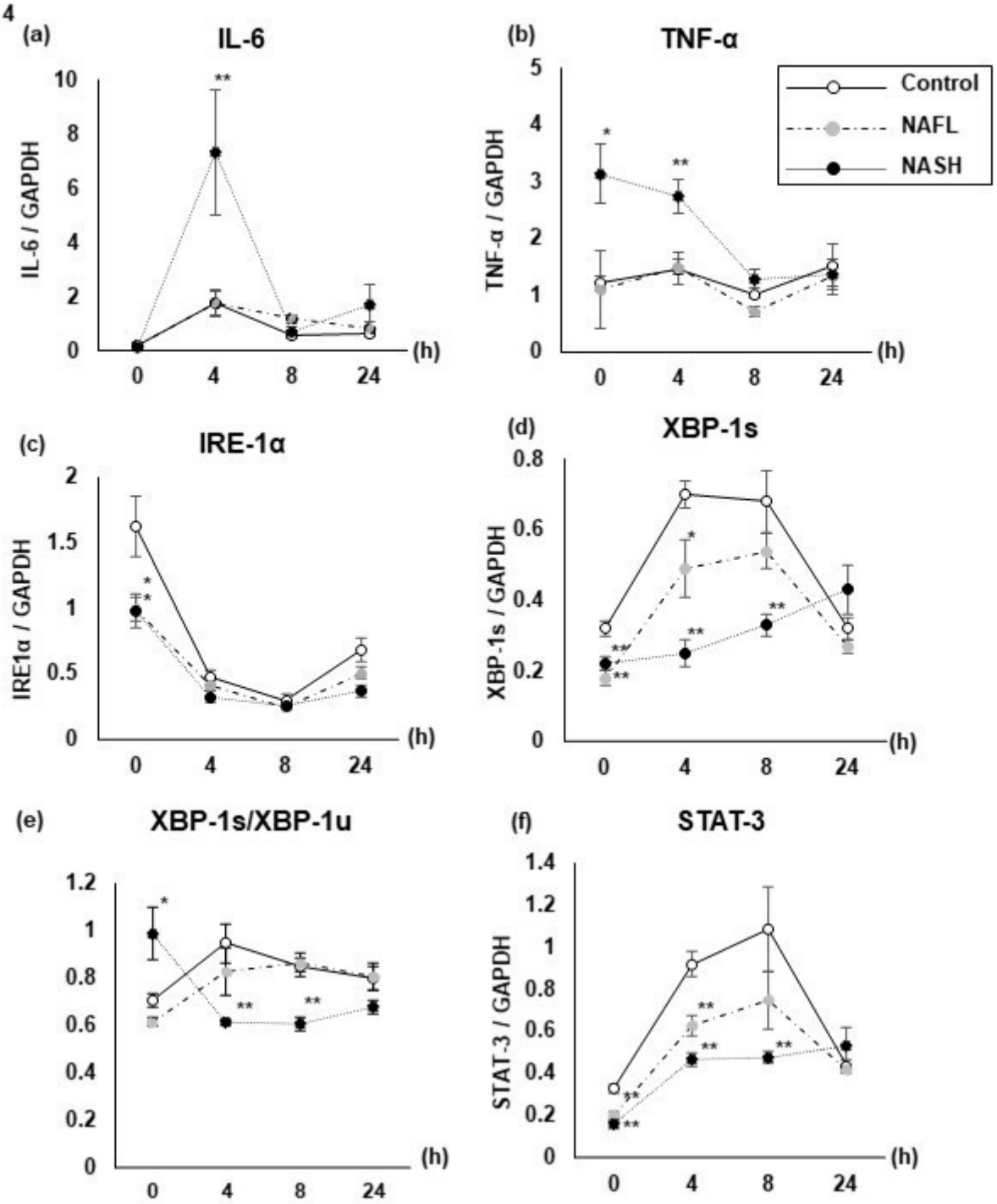

JHBP_1142_4.JPG

Fig.5

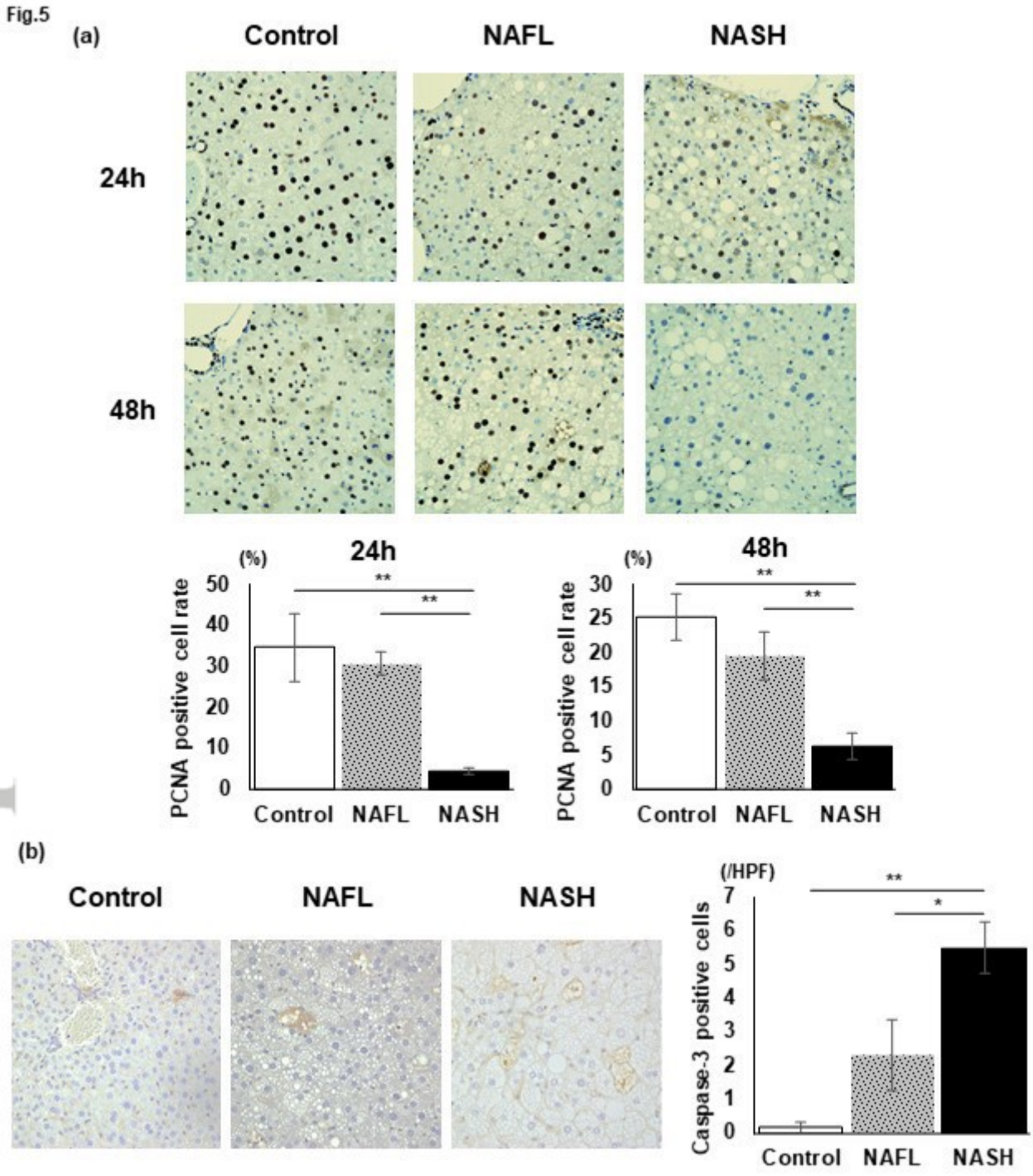

JHBP_1142_5.JPG

Fig.6

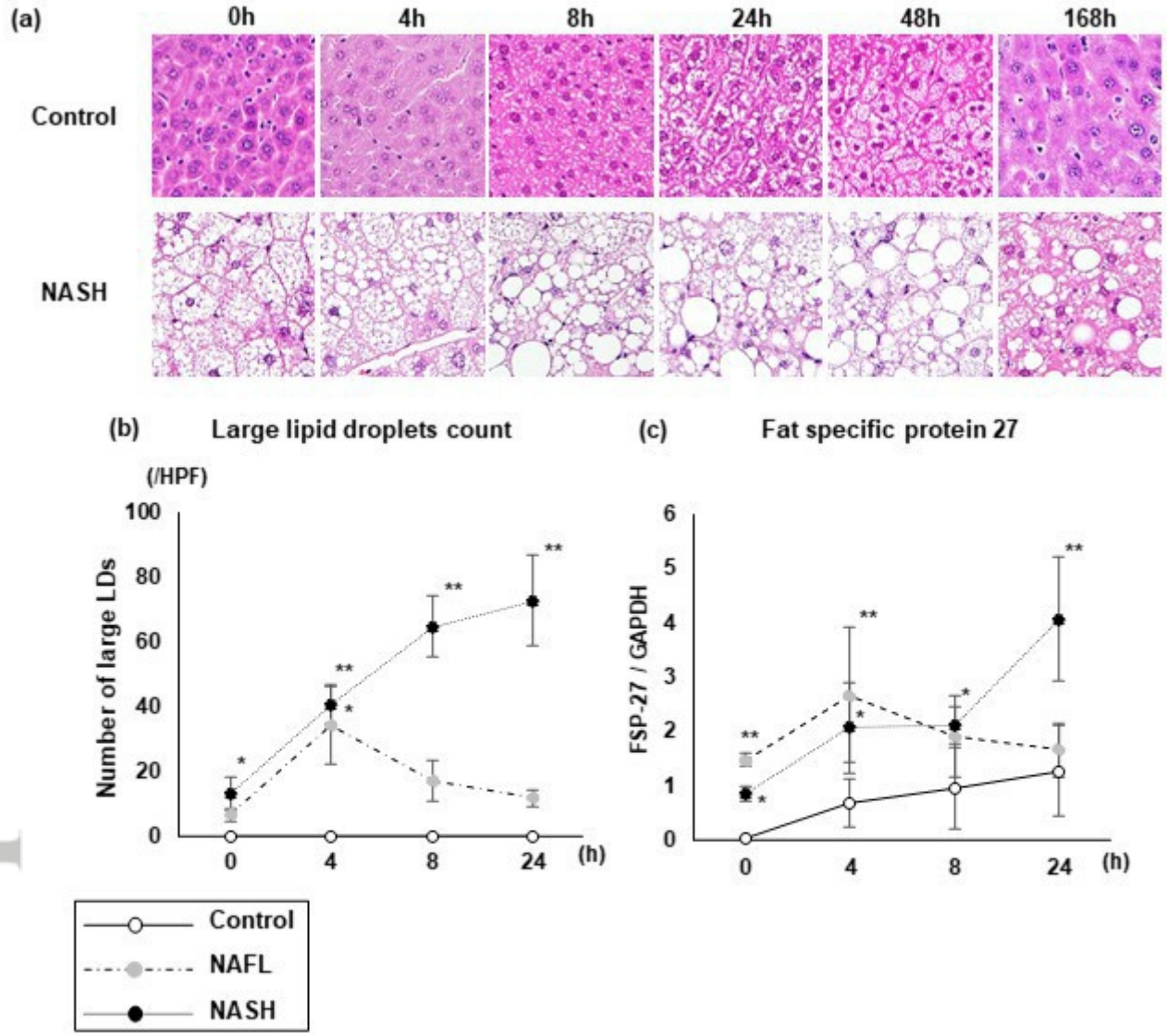

JHBP_1142_6.JPG